61 pages
DAA/Ames

A FINAL REPORT ON OPTICAL DIAGNOSTICS OF GAS-DYNAMIC FLOWS USING ADVANCED LASER MEASUREMENT TECHNIQUES

Polyatomics Proposal: NASA Ames Cooperative Agreement NCC 2-244

Prepared by: Kenneth P. Gross
Polyatomics Research Institute
1101 San Antonio Road, Suite 420
Mountain View, CA 94043

Submitted to: NASA Ames Research Center
Moffett Field, CA 94035

Date: July 17, 1985

(NASA-CR-176950) OPTICAL DIAGNOSTICS OF GAS-DYNAMIC FLOWS USING ADVANCED LASER MEASUREMENT TECHNIQUES Final Report, 1 Oct. 1983 - 31 Dec. 1984 (Polyatomics Research, Inc.) 61 p CSCL 20D G3/34

N86-30095

Unclas
43279

Andrew Komornicki

Director

PROGRESS REPORT NCC 2-244

Period: October 1, 1983 to December 31, 1984

Principal Investigator: Kenneth P. Gross

The first phase of the proposed research plan (see Polyatomics proposal A833-5 [KPG], "A Proposal on Optical Diagnostics of Gas-Dynamic Flows using Advanced Laser Measurement Techniques") has been successfully completed. Using laser-induced fluorescence to probe nitrogen flows seeded with small amounts of nitric oxide, simultaneous measurements of all three thermodynamic scalar quantities temperature, density, and pressure, have been demonstrated in a supersonic turbulent boundary layer. Instrumental uncertainty is 1% for temperature and 2% for density and pressure, making the technique suitable for measurements of turbulent fluctuations. This technology is currently being transferred to an experimental program (at Ames) designed to use these optical techniques in conjunction with traditional methods, to make unique measurements in turbulent flow-fields that have not been possible before. It is hoped that this work will make a significant impact on the present understanding of the physics of turbulence in contemporary fluid-dynamics research.

A detailed description of research progress and pertinent results will be found in the following articles and pre-prints of manuscripts that have been presented at technical meetings or submitted for publication in the scientific literature.

MANUSCRIPTS AND MEETING PAPERS

1. "Optical Stark Effect in the Two-Photon Spectrum of NO," accepted for publication in Physical Review Letters.

2. "Remote Measurements of Fluctuating Temperatures in a Supersonic Turbulent Flow using Two-Photon Laser-Induced Fluorescence," presented at the AIAA 17th Fluid Dynamics, Plasma Dynamics, and Lasers Conference, Snowmass, Colorado, June 25-27, 1984.

3. "Measurements of Fluctuating Temperatures in a Supersonic Turbulent Flow Using Two-Photon Laser-Induced Fluorescence," presented at the Conference on Lasers and Electro-optics, Anaheim, California, June 19-22, 1984.

4. "Measurements of Fluctuating Temperatures in a Supersonic Turbulent Flow using Laser-Induced Fluorescence," accepted for publication in American Institute of Aeronautics and Astronautics.

5. "Simultaneous Measurements of Fluctuating Temperature, Density, and Pressure in a Turbulent Flow Using Laser-Induced Fluorescence," presented at the International Conference on Lasers '84, San Francisco, California, November 26-30, 1984.

Optical Stark Effect in the Two-Photon Spectrum of NO

Winifred M. Huo[i]

Radiation Laboratory, University of Notre Dame, Notre Dame, IN 46556

and

Kenneth P. Gross[i][ii]

Stanford University, Stanford, CA 94305

and

Robert L. McKenzie

NASA Ames Research Center, Moffett Field, CA 94035

A large optical Stark effect has been observed in the two-photon spectrum $X^2\Pi \rightarrow A^2\Sigma^+$ in nitric oxide. It is explained as a near-resonant process in which the upper state of the two-photon transition is perturbed by interactions with higher-lying electronic states coupled by the laser field. A theoretical analysis is presented along with Stark parameters determined from ab initio wave functions. The synthetic spectrum reproduces the major experimental features.

PACS numbers: 33.55.+c, 33.80kn, 33.70Jg, 33.10-n

In this letter, we are reporting a quantitative determination of the optical Stark effect in a molecular, two-photon, electronic transition. In the past, optical Stark effects observed in resonant multiphoton transitions have been almost exclusively limited to atomic systems. Due to the high density of states, molecular Stark effects are expected to be more easily observed, especially in multiphoton transitions using high laser intensities. In fact, such observations have been reported recently.[1—8] However, previous analyses of Stark effects in molecular multiphoton transitions have been limited to order-of-magnitude estimates.

During the course of developing a laser-induced fluorescence technique for gas-flow diagnostics, two of us[4,5] have studied two-photon excitation of ro-vibronic transitions in the NO γ ($X^2\Pi$, $v''=0 \rightarrow A^2\Sigma^+$, $v'=0$) band. Unexpectedly large Stark broadening was observed in the spectrum, even at moderate laser intensities. Therefore, we have studied the Stark effect in some detail to understand the nature of the broadening mechanism.

The experimental arrangement used was described previously in Ref. 5. Selected regions of the $\gamma(0,0)$, two-photon, fluorescence-excitation spectrum were scanned with a dye laser, which was pumped by the third harmonic of a Nd:YAG laser operated at 10Hz. A linearly polarized beam was generated at wavelengths near 450nm, with a 5-nsec pulse duration, an average linewidth of $\approx$ 0.2 to 0.3 cm^{-1}, and with energies of a few mJ. The beam intensity distribution was spatially and temporally nonuniform, and varied from pulse to pulse. A large fraction of the beam energy was focused into a sample cell for the Stark measurements. Approximately 10% was split off and loosely focused into a reference cell to provide a simultaneous spectrum with negligible Stark broadening. NO pressures were identical in both cells and ranged from 0.05 to 0.1 torr, where collisional broadening

was negligible.

An example of the broadening for a spectral region in which the line separations are significantly greater than the laser bandwidth is shown in Fig. 1. The upper trace was taken using an average laser intensity of ≈ 3 GW/cm^2. The lower trace, recorded simultaneously with a reduced laser power level, shows a spectrum where the Stark effect is negligible. The upper spectrum displays an asymmetric shift to the blue for both the $S_{11}+R_{21}(20\frac{1}{2})$ and $S_{21}(16\frac{1}{2})$ transitions. The rotational sublevels, which are split by the laser field, are not resolved. The splitting appears in the spectrum as a broadening, 3 to 4 cm^{-1} wide. Additionally, the relative heights of the two peaks are reversed. Figure 2 shows a plot of the width (FWHM), of the $S_{11}+R_{21}(20\frac{1}{2})$ and $S_{11}+R_{21}(7\frac{1}{2})$ lines, as a function of the average laser energy. The width is linearly proportional to the pulse energy, indicating a quadratic Stark effect. The intercept at zero energy corresponds to the convoluted two-photon laser width and Doppler width.

To account for the observed Stark effect quantitatively, both shifts and widths induced by the optical field need to be considered. A survey of spectroscopic data for NO[6—8] shows that at the laser frequencies for the two-photon $X \rightarrow A$ transition, each rotational level of the A state is near-resonant with a one-photon transition to a J level of a high-lying discrete electronic state. The observed splitting can be attributed to near-resonant, one-photon coupling via the Stark field (i.e., a quadratic Stark effect). In addition to the splitting, a significant width is also introduced since the A state can be coupled with the ionization continuum by two-photon transitions, which are enhanced by the near-resonant one-photon step. This additional width corresponds to a quartic Stark effect.

An important factor in determining the magnitude of the observed Stark effect is the resonance-energy gap, G (the difference between the energies of the perturbing state and the sum of the A state and one-photon energies). From available experimental data,[6—9] the strongest perturbing level of the $S_{11}+R_{21}(20\frac{1}{2})$ branch has been identified as $B^2\Pi$, v=25; and for the $S_{21}(16\frac{1}{2})$ branch, $K^2\Pi$, v=1. Also, for the A state rotational levels considered, the smallest energy gaps vary between 3 and 4 cm^{-1}.

We have calculated the Stark shifts by solving the time-dependent Schrödinger equation directly. The commonly used perturbation approach[2,3] was found to be inadequate, owing to the small resonance-energy gaps. Calculations were performed for the combined molecule and field system with each rotational level of the A state coupled to six rotational levels of the $B^2\Pi$ or $K^2\Pi$ state, via dipole interactions; i.e., $J=J_A+1$, J_A, J_A-1 for each of the spin components, F_1 and F_2, of the perturbing state. Contributions from the $X^2\Pi$ state were negligible. In the dressed molecule representation,[10] we can cast the Schrödinger equation into the form of a secular equation.[11] For a state A, coupled to a set of bound states I and J, through the potential V, we have

$$\vec{G}+\vec{V}-\vec{a}=0 \tag{1}$$

where $G_{AA}=0$, $G_{IJ}=(E_I-E_A-\omega)\delta_{IJ}$, $V_{AA}=0$, and

$$V_{AI}=-\tfrac{1}{2}\mathcal{E}\mu_{AI}R(J_A,J_I,S_A,S_I,M) \tag{2}$$

Also, $V_{IJ}=0$, because these terms are nonresonant. In Eq. (2), μ_{AI} is the transition dipole moment, R is a rotational line shift factor, and $\mathcal{E}$ is the field strength. Associated with each eigenvalue, a_N, there is a dressed state wave function, $\Psi_N(\vec{r},t)$,

$$\Psi_N(\vec{r},t)=\left[B_{NA}(\Phi_A,n)+\sum_I B_{NI}(\Phi_I,n-1)\right]e^{-i[E_A+(n+\frac{1}{2})\omega-\alpha_N]t}, \qquad (3)$$

where Φ_A and Φ_I are the time-independent molecular eigenfunctions; B_{NA} and B_{NI} are time-independent coefficients; and n is a photon occupation number. The nonstationary wave function, $\Psi(\vec{r},t)$ is a linear combination of the Ψ_N's. For the case of two-state coupling,[12] our result agrees with that obtained previously in closed form.[13]

While $\Psi(\vec{r},t)$ is oscillatory, the laser probes only one of its components. Since a single laser field was used in this experiment, the probe and Stark frequencies are identical, and are always tuned to the component of $\Psi(\vec{r},t)$ with α closest to zero. We designate it as Ψ_o. The eigenvalue, α_o, then corresponds to the Stark shift observed. To determine α_o, Eq. (1) is solved separately for each M rotational sublevel. Since the experiment requires the Stark and probe frequencies to be equal, an iterative solution is required.

The rotational line shift factor, $\mathcal{R}$, is given by

$$\mathcal{R}(J_A,J_I,S_A,S_I,M)=\left(\frac{2J_A+1}{2J_I+1}\right)^{\frac{1}{2}}C(J_A1J_I,M0M)$$

$$\times\left[\sum_{\Omega_A=-\frac{1}{2}}^{\frac{1}{2}}\sum_{\Omega_I=-\frac{1}{2}}^{\frac{1}{2}}<A^2\Sigma^+,J_A\pm\tfrac{1}{2}\,|\,A^2\Sigma^+,\Omega_A>C(J_A1J_I,\Omega_A1\Omega_I)<^2\Pi,J_I\pm\tfrac{1}{2}\,|^2\Pi,\Omega_I>\right] \qquad (4)$$

Here we have assumed the use of a single, linearly polarized laser and intermediate coupling between Hund's case (a) and (b).

The two-photon rotational line strength, $S(J_X,J_A,S_X,S_A,M)$, between individual M levels of the $X^2\Pi$ and $A^2\Sigma^+$ states, determines the shape of the Stark spectrum. The

M-dependent line strength can be deduced from the unresolved two-photon rotational line strength of Halpern et al,[14] and is given by

$$S(J_X, J_A, S_X, S_A, M) = \frac{5 \mid C(J_A 2 J_X, M 0 M) \mid^2}{2J_X + 1} S(J_X, J_A, S_X, S_A). \qquad (5)$$

The Stark width for individual M levels, arising from the interaction of the wave function, Ψ_o, with the ionization continuum, is expressed by

$$\Delta\Gamma = \frac{\pi}{2} \sum_{\lambda} | < \Phi_{c,\lambda} \mid \vec{\mu} \cdot \vec{\mathcal{E}} \mid \Psi_o > |^2 . \qquad (6)$$

The continuum states $\Phi_{c,\lambda}$ are evaluated at energy, $E_C = E_A + 2\omega$, and the subscript, λ, sums over all degenerate quantum numbers. The M dependence of the widths is implicitly contained in rotational factors similar to $\mathcal{R}$. The energy shift, due to coupling to the continuum, was found to be negligibly small.

The vibronic transition moments, μ_{AI}, were calculated from ab initio wave functions, using a large (32σ, 22π, 6δ, 4ϕ) Slater-type basis set containing Rydberg functions.[11] Complete-Active-Space SCF calculations were carried out for the $A^2\Sigma^+$ state, followed by multireference, first-order, configuration-interaction (CI) calculations for both $^2\Sigma$ and $^2\Pi$ symmetries. Transition moments between the B, K states and the ionization continuum were calculated from discretized CI wave functions using the Stieltjes imaging method.

The Stark shifts and widths of the three rotational levels of the $A^2\Sigma^+$ state under consideration have been calculated for the experimental field intensity, I_{AV}, of 3 GW/cm^2, using a chaotic field model for the photon statistical behavior.[15] Their values are shown in Table I for representative M levels. Both the shifts and widths are strongly M-dependent, owing to a dominant M^2-dependent term in the rotational line shift factor. A synthetic,

Stark-broadened, two-photon spectrum of NO has been generated using the calculated parameters and is presented in Fig. 3. At a given probe frequency in the synthetic spectrum, all transitions that contributed to the intensity were convoluted with the laser and Doppler widths, using a Voigt function. The laser width was assumed to be composed of both probe and Stark fields, with an effective, single, Gaussian width of 0.5 cm^{-1}. The vertical lines in Fig. 3 represent the calculated positions of the Stark-shifted M level transitions at I_{AV}. The experimental spectrum taken at the same field strength is also reproduced in the figure. Comparing the two spectra, we find overall agreement. Both spectra show asymmetric shifts to the blue and a peak-height reversal from the weak-field case. The asymmetry is the result of M-dependent blue shifts and the intensity distributions of the shifted lines. The individual Stark widths smooth the line shape. The discrepancies between the experimental and synthetic spectra are probably due to uncertainties in the parameters used in the calculation. The effects of spectral, spatial, and temporal variations in the laser radiation were evaluated using both a time-dependent and spatially variant model, with either Lorentzian or Gaussian spectral distributions. In all reasonable cases, the changes to the synthetic spectral profiles, integrated over all time and space, were less than 10%. Finally, B_J and I_{AV} were varied over a reasonable range of uncertainties with only minor changes observed for the large M transitions.

In conclusion, a theoretical method has been developed that should be uniquely applicable to near-resonant Stark effects. Several aspects of the model were found to be essential for reproducing the experimental features in NO. In particular, the time-dependent Schrödinger equation had to be solved directly since perturbation methods were unsuccessful. Additionally, an iterative solution of the secular equation was necessary to

account for the single beam experiment properly.

(i) Mailing address: NASA Ames Research Center, Moffett Field, CA 94035.

(ii) Current affiliation: Polyatomics Research Institute, Mountain View, CA 94043.

[1] C.E. Otis and P. M. Johnson, Chem. Phys. Lett 83, 73 (1981).

[2] T. Srinivasan, H. Egger, H. Pummer, and C. K. Rhodes, IEEE J. Quantum Electron. QE19, 1270 (1983).

[3] B. Girard, N. Billy, T. Vigue, and J. C. Lehmann, Chem. Phys. Lett. 102, 168 (1983).

[4] R. L. McKenzie and K. P. Gross, Applied Optics, 20, 2153 (1981).

[5] K. P. Gross and R. L. McKenzie, Optics Letters 8, 368 (1983).

[6] E. Miescher and K. P. Huber, *Spectroscopy*, edited by D. A. Ramsay, M. T. P. International Review of Science Physical Chem., 1976, Ser. Two, 3.

[7] T. Ebata, N. Mikami, and M. Ito, J. Chem. Phys. 78, 1132 (1983).

[8] T. C. Steimle and H.-T. Liou, Chem. Phys. Lett. 100, 300 (1983).

[9] R. Gallusser and K. Dressler, J. Chem. Phys. 76, 4311 (1982).

[10] C. Cohen-Tannoudji and S. Reynaud, J. Phys. *B*10, 345 (1977).

[11] W. M. Huo, K. P. Gross, and R. L. McKenzie, NASA TM-85964 and unpublished work.

[12] S. H. Autler and C. H. Townes, Phys. Rev. 100, 703 (1955).

[13] L. D. Landau and E. M. Lifshitz, *Quantum Mechanics*, Pergamon Press, London, 1958, p. 143.

[14] J. B. Halpern, H. Zacharias and R. Wallenstein, J. Mol. Spectrosc. 79, 1 (1980).

[15] P. Zoller and P. Lambropoulos, J. Phys. *B*13, 69 (1980).

Table I. Stark shifts(cm^{-1}) and widths(cm^{-1}) calculated for three rotational levels of the $A^2\Sigma^+$, v=0 state at I_{AV} = 3 GW/cm^2

	F_1, J=22½		F_2, J=21½		F_2, J=18½	
M	Shift	Width	Shift	Width	Shift	Width
½	-0.03	0.06	-0.41	0.89	-0.02	0.04
5½	0.99	0.42	-0.25	0.85	1.02	0.70
10½	2.44	0.52	0.22	0.27	2.41	0.91
15½	3.83	0.49	1.11	0.21	3.87	0.93
20½	5.03	0.46	2.53	0.20	—	—

Figure captions

Figure 1 . Experimental two-photon spectra of NO: $X^2\Pi$, $v''=0 \rightarrow A^2\Sigma^+$, $v'=0$, S_{11} + $R_{21}(20\frac{1}{2})$, and $S_{21}(16\frac{1}{2})$ transitions at low and high laser intensities. NO pressure was 0.1 torr.

Figure 2 . Linewidth (FWHM) of the $S_{11}+R_{21}(20\frac{1}{2})$ and $S_{11}+R_{21}(7\frac{1}{2})$ lines as a function of laser energy. Focused beam diameter was $\approx$ 300 μ. NO pressure was 0.05 torr.

Figure 3 . Comparison of the Synthetic (———) and experimental (—) high-field spectra (same conditions as Fig. 1). The vertical lines represent the calculated positions of the shifted M levels.

Fig. 1

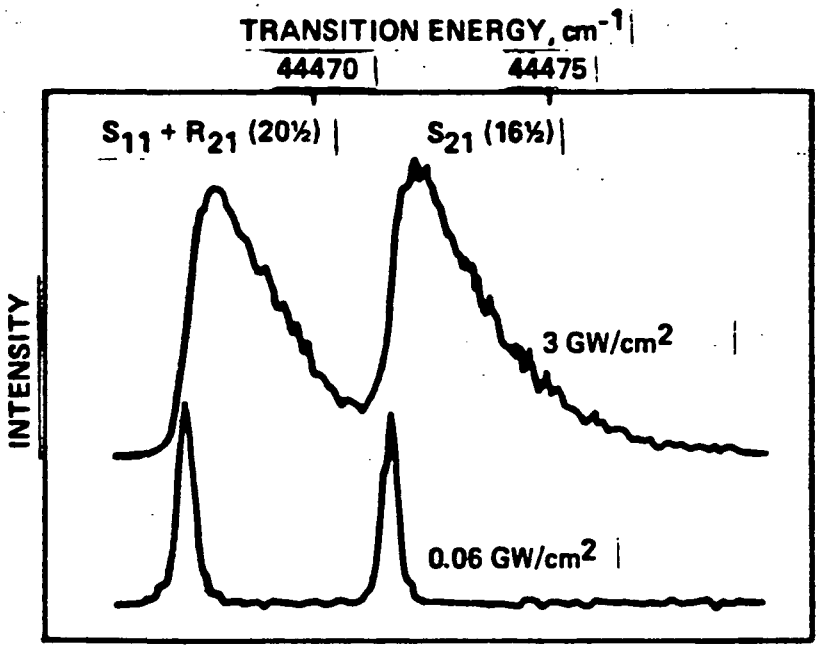
TRANSITION ENERGY, cm-1
44470
44475
S11 + R21 (20½)
S21 (16½)
INTENSITY
3 GW/cm2
0.06 GW/cm2

Fig 2.

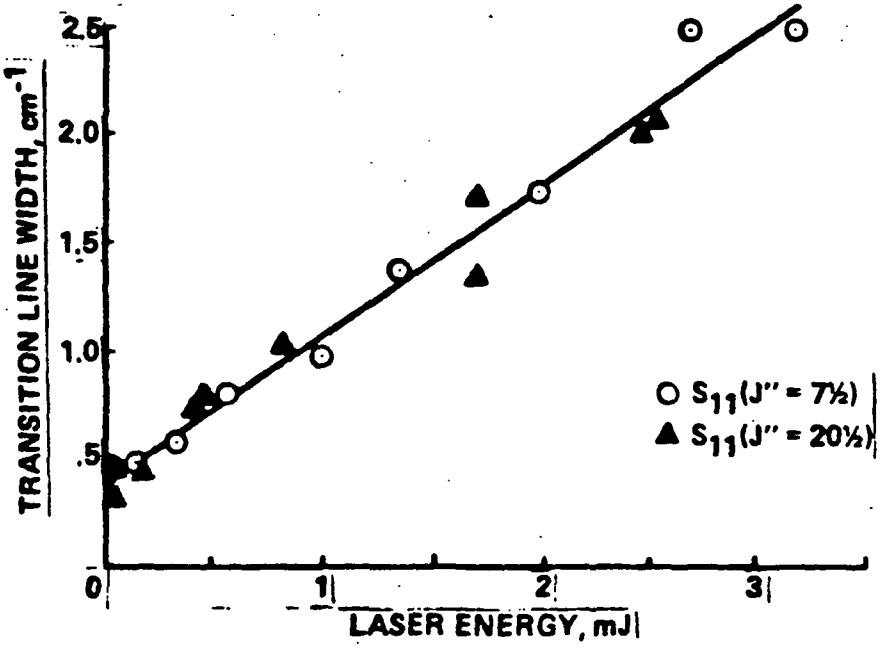
TRANSITION LINE WIDTH, cm⁻¹
2.5
2.0
1.5
1.0
.5
0
1
2
3
LASER ENERGY, mJ
O S11(J" = 7½)
▲ S11(J" = 20½)

Fig. 3

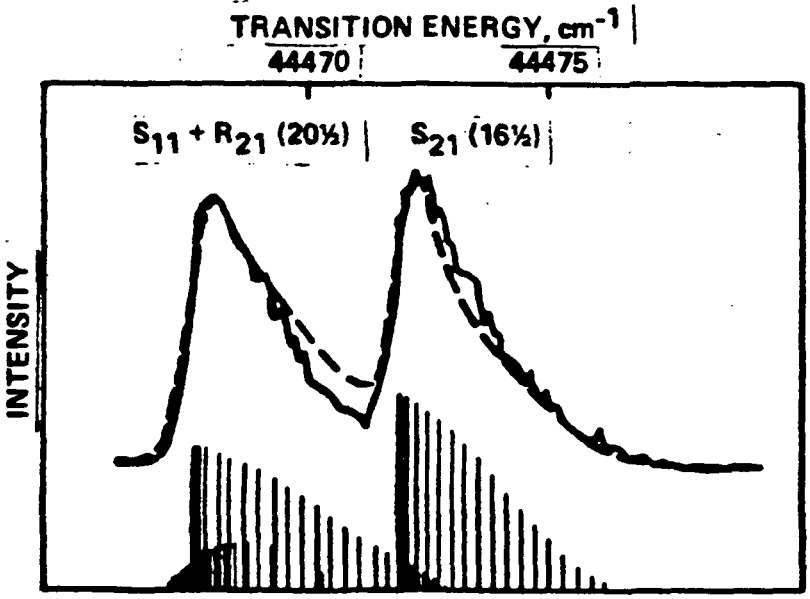
TRANSITION ENERGY, cm⁻¹
44470
44475
S11 + R21 (20½)
S21 (16½)
INTENSITY

Remote Measurements of Fluctuating Temperatures in a Supersonic Turbulent Flow Using Two-Photon Laser-Induced Fluorescence

by

K.P.Gross

Polyatomics Research Institute, 1101 San Antonio Rd., Suite 420, Mountain View, CA., 94043

and

R.L.McKenzie

NASA Ames Research Center, N-229-1, Moffett Field CA., 94035

A laser-induced fluorescence (LIF) technique has been developed that provides a practical means of nonintrusively measuring the fluctuating temperatures in low-temperature turbulent flows. In this paper, we review the capabilities of the method and report its application to a simple two-dimensional turbulent boundary layer flow at Mach 2. We show the results of remote measurements of the average temperature distribution through the boundary layer and the magnitudes of temperature fluctuations about their average values. To our knowledge, these data are the first of their kind obtained by nonintrusive means with spatial and temporal resolution adequate for turbulent boundary layer analyses.

The method, described in detail previously(1), requires that the flow be seeded with a low concentration of nitric oxide (NO). It relies on the ultraviolet fluorescence following two-photon excitation of two ro-vibronic transitions in the NO Gamma band. Each excitation is induced by a separate tunable dye laser tuned to the transition of interest. The two dye lasers are pumped by a common Nd:YAG laser but at slightly separated times following each pump

laser pulse. The subsequent double-pulse waveforms depicting the combined broad-band fluorescence from both excitations are then recorded, normalized by similar data from a non-flowing reference cell at known temperature, and related to the rotational temperature of the ground-state NO molecule. The rotational temperature of NO is taken to be closely coupled to the kinetic temperature of the gas mixture, thus providing a temperature measurement with each pump laser pulse. The temporal resolution of the measurement is approximately 125 nsec and it is obtained within a sample volume having dimensions less than 1 mm.

The windtunnel used for these experiments is a small blowdown facility that is capable of handling toxic gases such as NO. Nitric oxide concentrations up to 300 ppm were used, mixed with dry nitrogen. The test section is a rectangular Mach 2 nozzle with a 25 X 64 mm exit, followed by a slightly diverging channel, 762 mm in length from the nozzle throat to the optical ports. Optical access to the flow for the lasers was obtained through 50 mm diameter quartz windows on each side of the channel while fluorescence was observed through a similar window in the top of the channel. At a stagnation pressure of 3.5 atmospheres, the test section contained a fully-turbulent boundary layer filling the upper and lower thirds of its 33 mm height and had an inviscid core flow in the center.

The optical arrangement is illustrated in Fig. 1. Two grating-tuned dye lasers are simultaneously pumped at 10 Hz by the third-harmonic output of an Nd:YAG laser. The portion of the 355 nm pump beam directed to the second dye laser was optically delayed, giving a temporal separation of 125 nsec between dye laser pulses.

The first and second dye lasers were tuned, respectively, to

the J"=19 1/2 and J"=7 1/2, S11+R21 two-photon transitions in the NO Gamma(0,0) band. The two beams were combined collinearly, focused by a common 500 mm focal length lens, and partitioned into the windtunnel and reference paths. The focal spot size was about 0.5 mm.

The broad-band fluorescence from both the windtunnel and the reference cell was collected with nearly identical f/1 fused silica optics, nominally filtered with UV transmitting short-wave-pass filters, and imaged through apertures that limited observation of both sample volumes to a 1 mm region centered on the laser beam focal point. The fluorescence waveforms from each source were detected by solar-blind photomultipliers sensitive in the spectral range 225-330 nm and recorded by Tektronix 7912AD transient digitizers interfaced to an HP-1000 computer.

As described in Ref. 1, the data analysis leading to a temperature value for each pump laser pulse requires knowing the ratio of broad-band fluorescence energies resulting from each excitation. The ratio is obtained from each double-pulse waveform by fitting it to a six-parameter function derived for an exponentially decaying emitter driven by an excitation pulse with a Gaussian temporal profile. The two pulses in each waveform are then deconvolved and their individual integrals computed. The integral of each pulse is assumed to be linearly proportional to the total fluorescence energy resulting solely from its corresponding laser excitation, with account taken of the laser spectral width and all collision-broadened molecular transitions falling within the excitation bandwidth.

Figure 2 shows an overlay of some experimental waveforms and

their functional fits. In each example, the first pulse results from excitation of the J"=19 1/2 transition using excitation energies in the range from 1.5 to 2.0 mJ. The second pulse is from excitation of the J"=7 1/2 transition using approximately 0.5 mJ. Under these conditions, the noise seen in the waveforms is due principally to photon statistics with signal-to-noise ratios in the range of 25-50 for the windtunnel and 50-100 for the reference cell.

Prior to its windtunnel application, the instrumental uncertainty of the method was evaluated in a cooled non-flowing cell at conditions duplicating those expected in the windtunnel. The cell contained thermocouples located close to the laser sampling point that provided an independent measurement of the local temperature in the gas mixture. A comparison of temperature measurements in the cell over the range 155-295 K are shown in Fig. 3. The average temperatures calculated from 50 laser pulses are represented by the symbols. The error bars indicate the corresponding RMS deviation from each average value. Generally, the average spectroscopic temperatures agree with the thermocouples to within +/- 2 %, whereas the single-pulse temperatures varied between 2.5-4.0 % RMS for each data set.

The results of preliminary windtunnel measurements are illustrated in Figures 3 and 4. Figure 3 shows the variation of average temperatures obtained by the LIF technique as the measurement point is traversed from the channel centerline to a position approximately 0.7 mm from the wall. The filled symbols represent averages accumulated during 15 second runs with account taken of the declining stagnation temperature that is characteristic of all blowdown windtunnels. The open symbols are temperatures

implied from a pitot probe survey at the same conditions. The LIF average temperatures agree with the pitot values within +/- 2 % at all locations.

Figure 4 compares the RMS magnitudes of temperature fluctuations obtained by the LIF technique with similar measurements made using hot-wire probes in the same channel (open symbols) and with hot-wire measurements in a larger facility at similar conditions (dashed line). At this time, the cause of the apparent lack of agreement is unclear but the LIF measurements are judged to be less subject to interpretation than those from the intrusive hot-wire probes.

We believe that this nonintrusive laser-induced fluorescence technique offers new opportunities in basic turbulent flow research by providing measurement capabilities that were not possible previously. We have strong indications from other laboratory results that we will soon be able to extend it to include simultaneous temperature and density measurements, thus allowing pressure fluctuations to be obtained nonintrusively.

1. R.L.McKenzie and K.P.Gross, Two-Photon Excitation of Nitric Oxide Fluorescence as a Temperature Indicator in Unsteady Gasdynamic Processes , Appl. Optics, 20 ,2153,(1981)

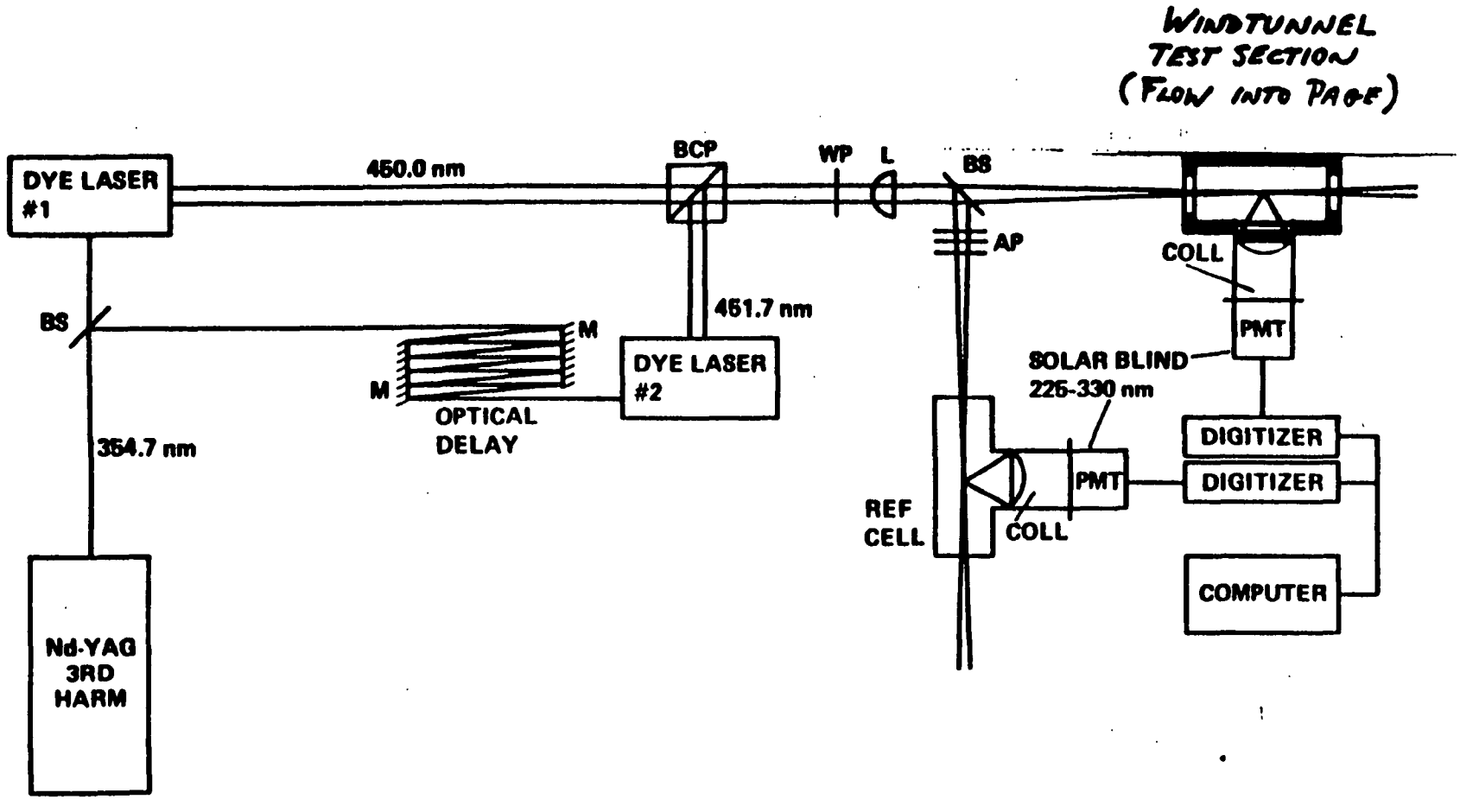

Fig. 1. Schematic of the experimental arrangement: BCP, beam-combining polarizer cube; WP, half-wave plate; L, lens; BS, beamsplitter; M, mirror; AP, attenuation plates; COLL, collection system; PMT, photomultiplier.

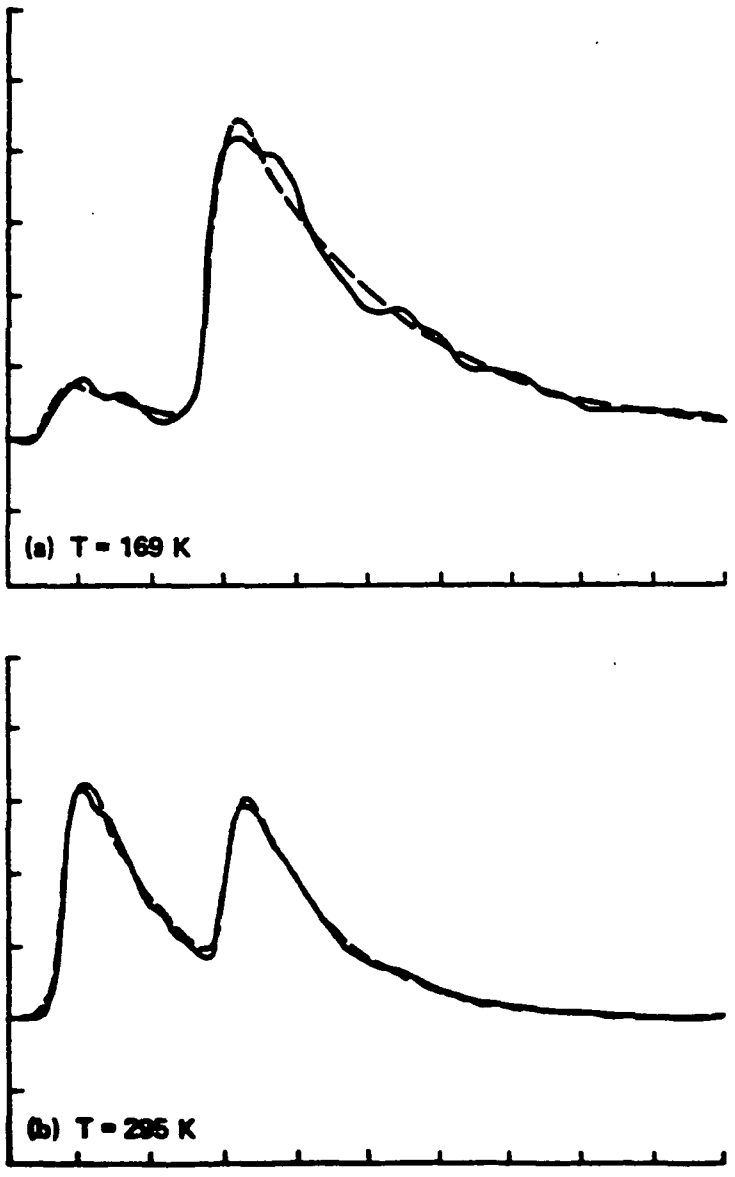

Fig. 2. Dual-pulse fluorescence waveform (solid line) and computer-fitted function (dashed line): (a) cold sample cell with 300 ppm NO in 0.5 atm N_2; (b) room-temperature reference cell with 1200 ppm NO in 0.5 atm. N_2. First pulse is fluorescence from the $S_{11} + R_{21}(19\ 1/2)$ excitation; second pulse is from the $S_{11} + R_{21}(7\ 1/2)$ excitation. Vertical amplifier bandwidth, 20 MHz; sweep, 50 nsec/div.

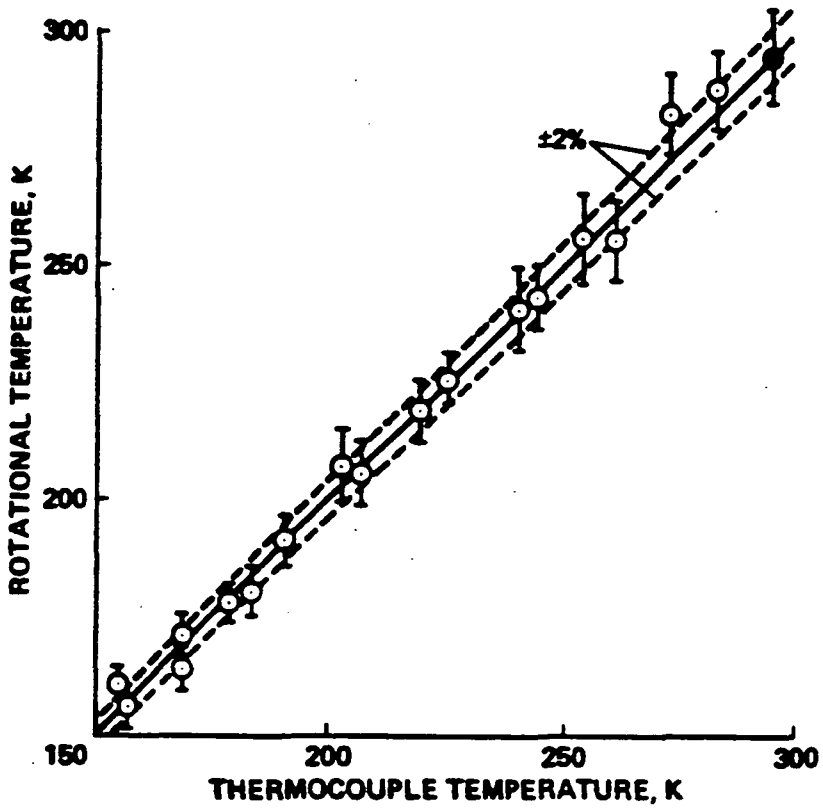

Fig.3 Comparison of measured rotational temperature and thermocouple temperature. Cell mixture: 300 ppm NO in 0.5 atm. N_2.

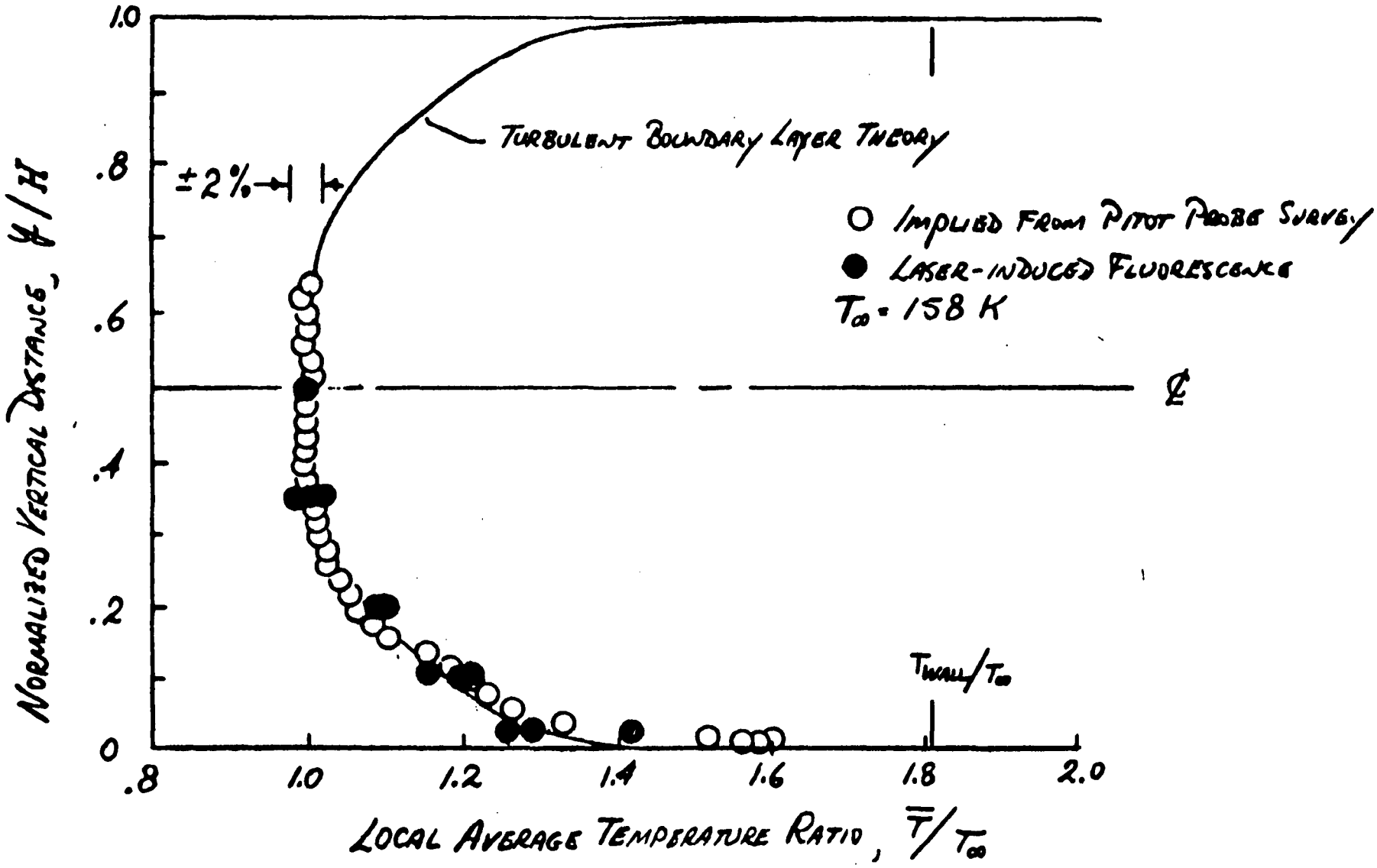

FIGURE 4. AVERAGE TEMPERATURE DISTRIBUTION IN A MACH 2.0 CHANNEL

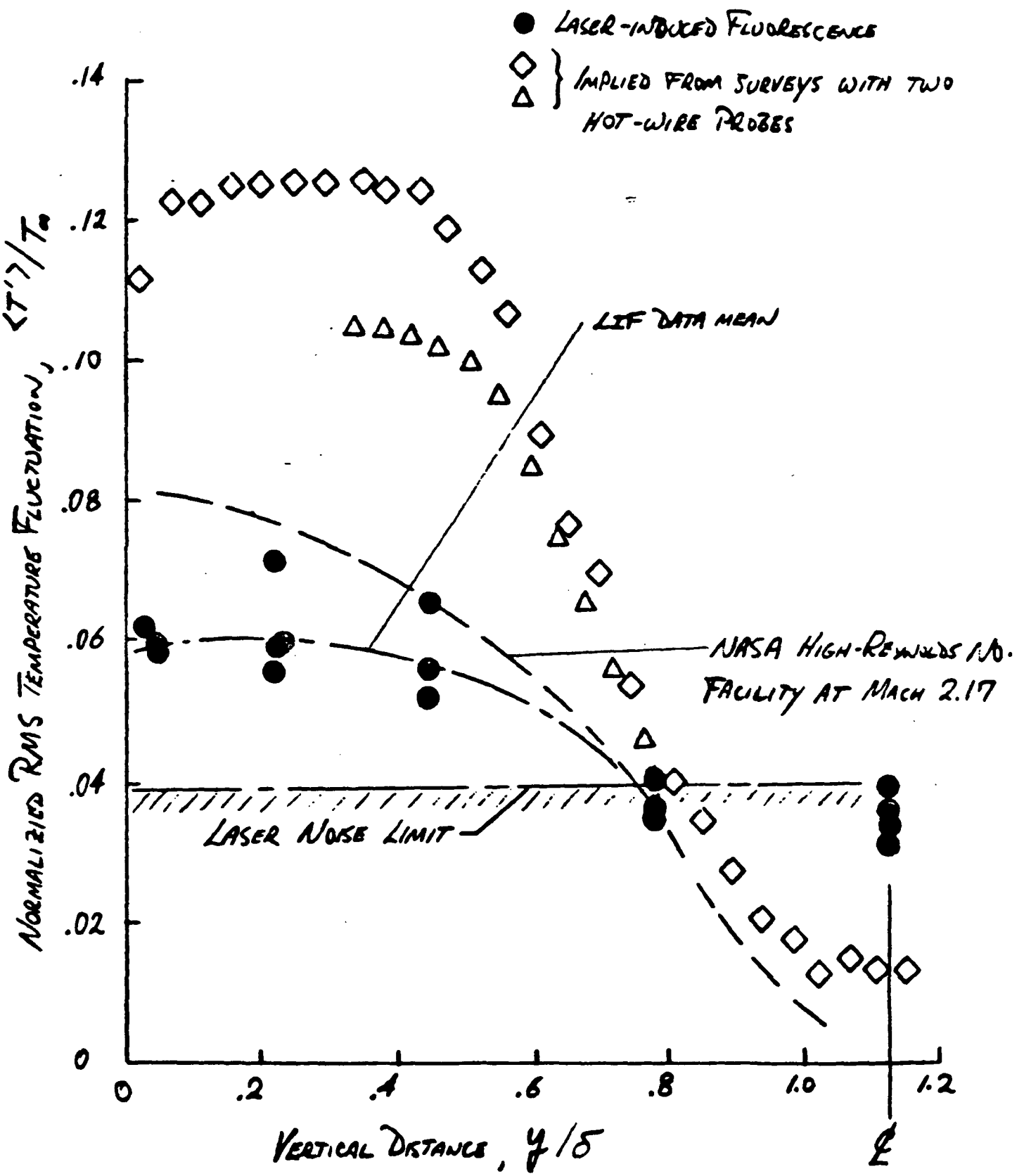

FIGURE 5. TEMPERATURE FLUCTUATIONS IN A MACH 2.0 CHANNEL

"MEASUREMENTS OF FLUCTUATING TEMPERATURES IN A SUPERSONIC TURBULENT FLOW USING TWO-PHOTON LASER-INDUCED FLUORESCENCE"

K. P. Gross, Polyatomics Research Institute, 1101 San Antonio Rd., Suite 420, Mountain View, California 94043, (415) 965-6255; and R. L. McKenzie, NASA Ames Research Center, MS 229-1, Moffett Field, California 94035, (415) 965-6158.

ABSTRACT

A technique for making instantaneous temperature measurements has been demonstrated in a turbulent boundary layer flow at Mach 2. The method relies on the laser excitation of ro-vibronic transitions in nitric oxide seeded gas mixtures.

SUMMARY:

"Measurements of Fluctuating Temperatures in a Supersonic Turbulent Flow using Two-Photon Laser-Induced Fluorescence"

K. P. Gross, Polyatomics Research Institute, 1101 San Antonio Rd., Suite 420, Mountain View, California 94043, (415) 965-6255; and R. L. McKenzie, NASA Ames Research Center, MS 229-1, Moffett Field, California 94035, (415) 965-6158.

A laser-induced fluorescence (LIF) technique has been developed that provides a means for non-intrusive measurements of fluctuating temperatures in low-temperature turbulent flows. In this presentation we describe the capabilities of the method and its application to a simple two-dimensional turbulent boundary layer flow at Mach 2. To our knowledge these data are the first of their kind obtained by non-intrusive means with spatial and temporal resolution adequate for turbulent boundary layer analyses.

The method and experimental arrangement is similar to that described previously [1,2], and requires that the flow be seeded with a low concentration of nitric oxide (NO). The technique relies on the ultraviolet fluorescence following two-photon laser excitation of two ro-vibronic transitions in the NO Gamma band. The rotational temperature of the NO is taken to be closely coupled to the kinetic temperature of the gas mixture, therefore providing a temperature measurement with each pump laser pulse. The temporal resolution of the measurement is approximately 125 nsec and it is obtained within a sample volume having dimensions less than 1mm.

The wind tunnel used for these experiments is a small blow-down facility capable of handling toxic gases such as NO. Nitric oxide concentrations up to 300 ppm were used, mixed with nitrogen. Optical access to the flow was obtained through 50 mm diameter fused silica windows on each side of the test channel while fluorescence was observed through a similar window in the top of the channel. At stagnation conditions of 3.5 atmospheres and ambient temperature, the test section contained a fully turbulent boundary layer which filled the upper and lower thirds of its 33 mm height. The center third contained an inviscid core flow at Mach 2.

Single-shot temperature measurements were made at a series of points from the centerline and thru the boundary layer to a position approximately 0.5 mm from the wall. The data acquisition rate during a 13 sec run time was 5 Hz, correspondig to 65 individual time-dependent temperature determinations. The average temperature distribution thru the boundary layer, obtained by the LIF measurements, was compared with the expected temperature profile implied from a pitot probe survey at the same conditions. Agreement was within $\pm$2% at all locations.

The instantaneous temperature measurement sensitivity varied between 3 - 4% rms for any given run, in agreement with previous measurements performed in a low temperature static test cell.[2] A discussion of the rms magnitudes of the temperature fluctuations in the turbulent boundary layer will be presented,

along with a comparison of the LIF data with invasive measurements of the turbulence intensity deduced from hot-wire probes.

Details of the experimental techniques, and refinements to improve S/N sensitivity as well as extending the capability of the method to include simultaneous temperature and density measurements will also be reported.

REFERENCES

1. R. L. McKenzie and K. P. Gross, Appl. Opt. 20, 2153 (1981).
2. K. P. Gross and R. L. McKenzie, Opt. Lett. 8, 368 (1983).

MEASUREMENTS OF FLUCTUATING TEMPERATURES IN A SUPERSONIC TURBULENT FLOW USING LASER-INDUCED FLUORESCENCE

Kenneth P. Gross*

Polyatomics Research Institute, Mountain View, California

Robert L. McKenzie†

NASA Ames Research Center, Moffett Field, California

Abstract

A laser-induced fluorescence technique has been developed that provides a practical means of nonintrusively measuring the instantaneous temperatures in low-temperature turbulent flows. It relies on the fluorescence from small concentrations of NO in a flow of N_2. The technique has been demonstrated in a two-dimensional turbulent boundary-layer at Mach 2. Both single-photon and two-photon excitation methods were used, but limits imposed on the two-photon method by Stark effects rendered it less accurate. Single-pulse measurements, in flows with 100 ppm NO, were obtained in the range from 150 to 295 K with an uncertainty of 1% rms. Fluctuations up to 6% rms were observed, owing to the turbulent flow. The average temperature distribution through the boundary-layer agreed well with temperatures implied by pitot-probe data.

Presented at the AIAA 17th Fluid/Plasma Dynamics and Laser Conference, Snowmass, Colo., June 25-27, 1984.

*Research Scientist.

†Research Scientist. Member AIAA.

Introduction

At the present time, few nonintrusive diagnostic methods have been demonstrated that have sufficient spatial and temporal resolution for accurately measuring the fluid-dynamic parameters of interest in low-temperature, compressible, turbulent flows. Except for velocity measurements using well established laser Doppler-velocimetry methods, most reported optical techniques are unable to resolve the turbulent fluctuations. Quantities such as temperature, density, and their correlation with velocity remain as important variables to be obtained for the experimental verification of turbulence models.

Time-resolved light scattering techniques using Rayleigh or spontaneous Raman processes have been applied to the measurement of temperature and density,[1-3] but the observation of turbulent fluctuations is typically made difficult by one or more sources of background noise. For the case of Rayleigh scattering,[4,5] the signal is at the same frequency as the laser, requiring the careful rejection of stray light. The presence of particulates in the flow can easily confuse the signal analysis. Single-pulse Raman measurements have been reported,[6] but the small Raman scattering cross-section, typical of all common gases, leads to very weak signals. Laser pulse energies approaching 1 Joule are required to achieve the signal-to-noise ratios necessary to resolve fluctuations owing to turbulence. Modern nonlinear Raman processes, such as coherent anti-Stokes Raman scattering (CARS),[7] have also been applied to turbulent flows, but primarily in high-temperature combustion environments where molecular vibrational temperatures can be used as an indicator of the bulk gas temperature.

In this paper, a method is described that is based on the strong and frequency-shifted signals from laser-induced fluorescence (LIF). The keystone to implementing such a method is the identification of a fluorescent species with spectroscopic features that are resonant with available laser frequencies, and with chemical behavior that is compatible with the operating requirements of an aerodynamic flow facility. Species that are corrosive, reacting, or condense in an expanding flow are usually impractical in most aerodynamic research applications. LIF techniques have been reported[8-11] that are based on a variety of species with practical application to particular experimental situations. However, most use either a transient species, such as OH, that is available only in high-temperature combustion flows, or they rely on materials that tend to condense at the low temperatures of most supersonic wind tunnel flows.

An excellent candidate for use in aerodynamic research is nitric oxide (NO). Its chemical stability, in combination with strong spectroscopic features that are accessible by commercially available lasers, make it a practical seed gas for the applications addressed here. Conversely, the gas is toxic, requiring it to be used in very dilute concentrations; and it will oxidize in air, limiting its use in air flows. However, we show that in N_2, it allows nonintrusive measurements of temperature in flows of interest that are not now possible by any other means.

The sensitive measurement of temperature in turbulent and low-temperature flows requires several further considerations regarding the spectroscopic attributes of the fluorescent species. Those of primary importance include: (1) the presence of absorbing and fluorescing transitions with sufficient strength to provide low-noise signals, (2) spectral features that can be resolved with sufficient detail to accurately infer a temperature, and (3) the

availability of sufficient information to accurately account for the effects of fundamental molecular processes affecting the fluorescence signals, such as collisional quenching and transition spectral broadening. Most of these processes are dependent on temperature and density, and their variation in a turbulent flow must be included in the signal analysis. In addition, to obtain accurate spectroscopic measurements of temperatures below 500 K, the use of resolved rotational line spectra is most often required because only rotational energy differences are smaller than, or comparable to, the thermal energy being measured. An attractive feature of NO is that it is a diatomic molecule, with simply-analyzed rotational spectra, that satisfies all of the requirements above.

The measurement technique applied here is similar to that described previously.[12,13] It relies on the detection of broad-band ultraviolet (UV) fluorescence following laser excitation of two transitions originating from different rotational states in the $NO(X^2\Pi, v''=0 \rightarrow A^2\Sigma^+, v'=0)$ vibronic band. Since the fluorescence energy following each excitation is proportional to the energy absorbed by the gas for each transition, and that in turn is proportional to the initial-state number densities, the ratio of fluorescence energies for the two transitions can be related to the rotational temperature of the ground-state NO molecules through the Boltzmann equation. In its simplest form, the relation is:

$$\frac{I_2}{I_1} = \frac{n_2}{n_1} = \exp\left[\frac{-(E_2 - E_1)}{kT}\right] \qquad (1)$$

where I_i is the fluorescence intensity from transitional i, n_i is the initial-state number density, E_i is the initial-state rotational energy, k is the Boltzmann constant, and T is the rotational temperature. The

rotational temperature is assumed to be closely coupled to the kinetic temperature of the gas mixture so that the two remain equal for all flow conditions of practical interest.

Equation (1) is used in conjunction with the assumption that all radiative and non-radiative decay rates of the upper states populated by each laser excitation, or by the re-distribution of energy among upper states prior to decay, are equal. For the upper electronic state of $NO(A^2\Sigma^+, v'=0)$, quenching rates and fluorescence lifetimes are known to be insensitive to rotational quantum number[14,15] and, hence, are nearly equal for all rotational transitions observed in the broad-band fluorescence emission. Consequently, the degree of rotational re-distribution preceding the emission is not important if fluorescence is observed from all rotational transitions in a given vibronic band. Since the rates are nearly equal, their ratio is near unity and they have no influence on Eq. (1).

Fluorescence excitation may be accomplished at laser frequencies that are resonant for either single-photon or two-photon absorption. In the latter case, the molecules absorbs two photons with frequencies at half the transition frequency. The two rotational transitions necessary for Eq. (1) are excited using two independent, tunable, lasers. The pulses from each laser are separated slightly in time, allowing the fluorescence from both to be recorded simultaneously with a single detection system. Subsequent deconvolution of the double-pulse waveforms then leads to the ratio of fluorescence energies. Measurements are made simultaneously in both the turbulent wind tunnel flow and in a non-flowing reference cell at known temperature and pressure. The reference cell signals are used to normalize the variations in wind tunnel signals, owing to pulse-to-pulse fluctuations in laser energy and spectral frequency.

Experimental Method

Wind Tunnel

The flow facility used for these experiments is a small blowdown wind tunnel consisting of a high-pressure storage reservoir at ambient temperature, a supersonic-nozzle test section, and an evacuated dump tank. The facility can handle toxic gases such as NO at low concentration levels. Up to 300 ppm NO in nitrogen was used for the two-photon LIF measurements. The boundary layer studied was produced on the lower wall of a rectangular Mach 2 nozzle. Figure 1 shows a simple schematic of the boundary-layer channel and depicts the test-section instrumentation ports and collection optics geometry used for the fluorescence measurements. The nozzle has a 25 × 64-mm exit, followed by a slightly diverging channel that extends 762 mm from the nozzle throat to the measurement ports. The facility was operated at ambient total temperature with stagnation pressures ranging from 3 to 7 atm. At a stagnation pressure of 3.5 atm, the test section contained a fully turbulent boundary layer filling the upper and lower thirds of its 33-mm height with an inviscid core flow in the center. The test time varied between 5 and 20 sec, with the upper limit determined by reservoir stagnation pressure and dump-tank capacity. Optical access to the flow for the lasers was obtained through 50-mm-diam fused-silica windows mounted on each side of the channel. Fluorescence was observed through a similar window on the top of the channel. Static pressure measurements were made at the channel wall and a pitot tube was temporarily inserted through the top port in the test section to make extensive measurements of total pressure through the boundary layer. Shadowgraphs of the flow taken with and without the pitot tube in place indicated that the measurement volume was free from shock waves or other significant disturbances. The nominal test conditions were as follows.

Stagnation pressure, P_t = 3.5 atm

Mach number, M_∞ = 2.03

Stagnation temperature, T_t = 295 K

Free-stream temperature, T_∞ = 158 K

Boundary-layer thickness, δ = 1.4 cm

Reynolds number based on δ, $Re_\delta = 6 \times 10^5$

LIF Experiment

The optical arrangement used for the LIF measurements is illustrated in Fig. 2. Two grating-tuned dye lasers were pumped at 10 Hz by the 355-nm third-harmonic output of an Nd:YAG laser. The portion of the pump beam directed to the second dye laser was optically delayed, using two plane mirrors, giving a temporal separation of 130 nsec between the two 5-nsec dye-laser pulses. Each laser pulse was linearly polarized, and had an energy of a few millijoules contained in a spectral bandwidth of 0.2-0.3 cm^{-1}.

For two-photon LIF measurements, the first and second dye-laser pulses, at wavelengths near 450 nm, were tuned to half the transition frequencies corresponding to the J" = 19-1/2 and J" = 7-1/2, $\underset{\vee}{S11} + \underset{\vee}{R21}$, two-photon transitions, respectively. For single-photon measurements, each dye-laser output was frequency-doubled with potassium pentaborate (KB5) to produce UV energies of several microjoules. The single-photon transitions used were the J" = 18-1/2, $\underset{\vee}{Q11} + \underset{\vee}{P21}$ line and the J" = 7-1/2, $\underset{\vee}{R21}$ line. In both cases the orthogonally polarized beams were made collinear, focused by a common lens with a 500-mm focal length, and partitioned in the wind-tunnel test section and reference cell. The focal spot size at the measuring point was 0.5 mm.

Broadband nitric oxide fluorescence in the spectral range from 225 to 330 nm was collected from the flow channel and reference cell with nearly identical f/1 fused-silica optics. It was transmitted through broadband UV

filters (Schott UG-5) and imaged through an aperture that limited the observed sample volume to a 1-mm path length along the laser beam axis. Although reabsorption of the Y(0,0) emission was negligible in our experiments, the spectral cut-off of the filters blocked this band, thereby eliminating the influence of reabsorption on the temperature measurement.

The fluorescence waveforms were detected by solar-blind photomultipliers with peak responsivity in the ultraviolet, and recorded by Tektronix 7912AD transient digitizers interfaced to an HP-1000 computer. The fluorescence recording time was 500 nsec. During this time interval the interaction volume is convected downstream approximately 0.25 mm by the Mach 2 flow, and remained within the field of view of the imaging and detection system (Fig. 1b).

The effective temporal resolution for each instantaneous temperature measurement was determined by the 130-nsec separation of dye-laser pulses. Spatial resolution was determined by the nearly cylindrical sample volume of approximately 0.5 mm diam by 1.0 mm in length.

Before each wind-tunnel run, static fluorescence measurements were performed with the flow channel filled with the test gas mixture at ambient temperatures. These pre-run tests served to calibrate the measurement system, using the known pressures and temperatures in both the flow channel and reference cell. Gas pressure in the room temperature reference cell was adjusted so that Voigt line-shape profiles were matched to those in the wind-tunnel flow. The Voigt parameters were calculated using the data of Dodge et al.[16] Line-shape matching was accomplished by equating the normalized Voigt functions at line center. This procedure maximized the effectiveness for normalization of pulse-to-pulse variations in fluorescence signal amplitude owing to the unavoidable frequency jitter of each dye laser.

As described in Ref. 12, the data analysis leading to a temperature value for each pump laser pulse requires knowing the ratio of broadband fluorescence energies resulting from each excitation. The ratio is obtained from each double-pulse waveform by fitting it to a six-parameter function derived for an exponentially decaying emitter driven by a short excitation pulse with a Gaussian temporal profile. The two pulses in each waveform are then deconvolved and their individual integrals computed. The integral of each pulse is assumed to be linearly proportional to the total fluorescence energy resulting solely from its corresponding laser excitation, with account taken of the laser spectral width and all collision-broadened molecular transitions falling within the excitation bandwidth.

Figure 3 shows an example of some experimental fluorescence waveforms and their functional fits for typical wind-tunnel conditions using single-photon excitation. The first pulse results from excitation of the $J'' = 18\text{-}1/2$ rotational level, and the second pulse is from excitation of the $J = 7\text{-}1/2$ level. Ultraviolet laser energies were in the range of 1-3 μJ for each excitation. For an NO concentration of 100 ppm (fig. 3a), the photon-statistical noise is very low and the signal-to-noise ratios for each pulse were approximately several hundred to one. For the weaker signals at 5 ppm (Fig. 3b), the photon-statistical noise on the waveforms is evident and easily distinguished from the computer-fitted function. The experimental waveforms observed using two-photon excitation and 300 ppm NO had signal-to-noise ratios of about 25, also limited by photon-statistical noise.

Results

The instrumental uncertainty for the LIF measurements was initially evaluated in a low-temperature static test cell using two-photon

excitation.[13] Generally, the average spectroscopic temperatures agreed with the thermocouple to within ±2%, whereas the instantaneous single-shot temperatures varied between 3% and 4% rms for each data set, thus defining the instrumental rms noise sensitivity using two-photon excitation.

Two-photon excitation of the NO $\gamma(0,0)$ band, although easier and more convenient to implement experimentally than single-photon excitation, suffers from Stark broadening caused by the intense laser fields needed to induce appreciable absorption.[13,17] This effect, which manifests itself as a power-dependent broadening of the spectroscopic lines used for the measurement, defeats the use of normalization by a reference cell, and forces the measurements to be made using a minimum laser intensity with a corresponding decrease in signal-to-noise ratio. It is this basic limitation for the two-photon process that limits the temperature measurement noise to approximately 4%. By using single-photon excitation, much higher signal levels can be achieved with much lower laser intensities, giving the added advantage that Stark effects are completely negligible. The primary disadvantages accompanying the use of one-photon excitation are the need for a more complicated experimental setup and the rejection of scattered laser light at wavelengths close to those of the fluorescence signals. In larger scale flows, laser beam absorption along its path to the sample volume may also be troublesome. Fortunately, for NO $\gamma(0,0)$ band excitation and nitric oxide concentrations of 100 ppm or less, the optical transmission through the sample to the measurement point in these experiments was greater than 99%. Additionally, the single-photon-induced fluorescence signals were much larger than the stray light levels encountered, allowing adequate rejection of radiation at the excitation frequency with simple band-pass filters.

The higher signal levels produced using single-photon excitation also allow a considerable reduction in nitric oxide seeding concentration. Figure 4 is a plot of temperature sensitivity versus NO concentration, using UV laser energies of a few microjoules. It shows that for nitric oxide concentrations above 50 ppm in 0.5-atm N_2, the rms noise in the temperature measurement is about 1%. At concentrations below 50 ppm, the effects of photon-statistical noise begin to increase. Nevertheless, useful measurements can still be made at concentrations of only a few ppm, although interference from scattered laser light will become a larger fraction of the total signal and may require increased spectral filtering. Single-photon measurements using concentrations of about 1-2 ppm are nearly equivalent in noise sensitivity to the corresponding two-photon measurements made using 300-ppm NO.

The results of the wind-tunnel tests are illustrated in Figs. 5 and 6. Figure 5 shows the distribution of average temperature obtained by the LIF method, as the measurement point is traversed from the channel centerline to a position approximately 0.5 mm from the wall. Both one-photon and two-photon data are presented together and are shown by the solid symbols. They represent averages accumulated during 13-sec runs, with account taken of the declining stagnation temperature that is characteristic of blowdown flow facilities. The values plotted are the corresponding average temperatures after 2 sec from the start of the run. The data acquisition rate was limited by the digitizers to 5 Hz, corresponding to 65 temperature determinations per run. The open symbols are temperatures implied from a pitot probe survey at the same conditions, using the standard one-dimensional equations derived for isentropic compressible flow[18] and assuming that the total temperature and static pressure are constant through the boundary layer. The solid theoretical curve is a solution of the compressible, turbulent, boundary-layer

equations using a two-layer algebraic eddy-viscosity model.[19] Average temperatures determined using either one- or two-photon excitation are in agreement with one another and both agree with the pitot probe results to within ±2%.

Figure 6 depicts the rms magnitudes of the temperature fluctuations owing to turbulence, obtained by single-photon LIF for an NO concentration of 100 ppm. The total rms deviations have been corrected by removing the average instrumental noise of ≈1% determined from the static calibration runs, thus leaving only the fluctuating temperature component resulting from the local flow conditions. Run-to-run variations of the turbulence level determined at the same location in the boundary layer may be due in part to statistical uncertainties resulting from the limited number of data samples taken during a given wind-tunnel run.

Conclusion

Quantitative nonintrusive measurements of fluctuating temperatures using laser-induced fluorescence have been made in a simple, well-characterized, Mach 2, turbulent boundary-layer flow, seeded with 100-300 ppm of NO. Results obtained using both one-photon and two-photon NO $\gamma(0,0)$ rotational line excitation agree with average temperature profiles deduced from pitot-probe surveys to within 2%. The method using two-photon LIF has been shown to be much less sensitive for instantaneous measurements than the one-photon method, a result of optical Stark broadening caused by the high laser field intensities needed for the two-photon measurements. The application of one-photon LIF in this study has demonstrated the capability for directly measuring turbulent fluctuations of temperature as small as 1% of the average local value. Additionally, the one-photon technique remains fairly sensitive

at much lower NO concentrations, and could be effectively implemented in larger scale facilities where lower seeding levels are more desirable.

Work in progress in our laboratory indicates that the present method can most likely be extended to include simultaneous density measurements using an off-resonance excitation approach similar to that described for flow studies using iodine fluorescence.[9] This refinement would allow simultaneous measurements of temperature and density, thus providing nonintrusive pressure measurements.

Acknowledgments

The authors are grateful to D. J. Monson and P. Logan for providing the pitot tube measurements and boundary-layer calculations represented in Fig. 5.

References

[1]Peterson, C. W., "A Survey of the Utilitarian Aspects of Advanced Flowfield Diagnostic Techniques," AIAA Journal, Vol. 17, Dec. 1979, pp. 1352-1360.

[2]Lederman, S. and Sacks, S., "Laser Diagnostics for Flowfields, Combustion, and MHD Applications," AIAA Journal, Vol. 22, Feb. 1984, pp. 161-173.

[3]Trolinger, J. D., Azazzy, M., Modarress, D., and Craig, J. E., "Laser Diagnostic Methods/A Summary," AIAA Paper 83-1683, July 1983.

[4]Namer, I., Bill Jr., R. G., Talbot, L., and Robben, F., "Density Fluctuations in a Flame in a Karman Vortex Sheet," AIAA Journal, Vol. 22, May 1984, pp. 647-654.

[5]Gouldin, F. C. and Dandekar, K. V., "Time-Resolved Density Measurements in Premixed Turbulent Flames," AIAA Journal, Vol. 22, May 1984, pp. 655-663.

[6]Dibble, R. W., Kollmann, W., and Schefer, R. W., "Conserved Scalar Fluxes Measured in a Turbulent Nonpremixed Flame by Combined Laser Doppler Velocimetry and Laser Raman Scattering," presented at the 1982 Fall Meeting of the Western States Section of the Combustion Institute, Sandia National Laboratories, Livermore, Calif., Paper WSS/CI 82-52, October 11-12, 1982.

[7]Hall, R. J. and Eckbreth, A. C., "Coherent Anti-Stokes Raman Spectroscopy (CARS): Application to Combustion Diagnostics," in Laser Applications, J. F. Ready and R. K. Erf (eds)., Vol. 5, Academic Press, 1984, pp. 214-309.

[8]Lucht, R. P., Laurendeau, N. M., Drake, M. C., Lapp, M., and Pitz, R. W., "Single-Pulse, Laser-Saturated Fluorescence Measurements of OH in Turbulent Nonpremixed Flames," Optics Letters, Vol. 9, 1984, pp. 90-92.

[9]McDaniel, J. C., Baganoff, D., and Byer, R. L., "Density Measurement in Compressible Flows Using Off-Resonant Laser-Induced Fluorescence," Physics of Fluids, Vol. 25, 1982, pp. 1105-1107.

[10]Cheng, S., Zimmerman, M., and Miles, R. B., "Supersonic-Nitrogen Flow-Field Measurements with the Resonant Doppler Velocimeter," Applied Physics Letters, Vol. 43, 1983, pp. 143-145.

[11]Epstein, A. H., "Quantitative Density Visualization in a Transonic Compressor Rotor," Engineering for Power, Vol. 99, 1977, pp. 460-475.

[12]McKenzie, R. L. and Gross, K. P., "Two-Photon Excitation of Nitric Oxide Fluorescence as a Temperature Indicator in Unsteady Gasdynamic Processes," Applied Optics, Vol. 20, 1981, pp. 2153-2165.

[13]Gross, K. P. and McKenzie, R. L., "Single-Pulse Gas Thermometry at Low Temperatures Using Two-Photon Laser-Induced Fluorescence in NO-N_2 Mixtures," Optics Letters, Vol. 8, 1983, pp. 368-370.

[14]Nutt, G. F., Haydon, S. C., and McIntosh, A. I., "Measurement of Electronic Quenching Rates in Nitric Oxide using Two-Photon Spectroscopy," Chemical Physics Letters, Vol. 62, 1979, pp. 402-404.

[15]McDermid, I. S. and Laudenslager, J. B., "Radiative Lifetimes and Electronic Quenching Rate Constants for Single-Photon-Excited Rotational Levels of NO($A^2\Sigma^+$,v'=0)," Journal of Quantitative Spectroscopy and Radiative Transfer, Vol. 27, 1982, pp. 483-492.

[16]Dodge, L. G., Dusek, J., and Zabielski, M. F., "Line Broadening and Oscillator Strength Measurements for the Nitric Oxide $\gamma(0,0)$ Band," Journal of Quantitative Spectroscopy and Radiative Transfer, Vol. 24, 1980, pp. 237-249.

[17]Huo, W. M., Gross, K. P., and McKenzie, R. L., "Optical Stark Effect in the Two-Photon Spectrum of NO," to be published in Physical Review Letters.

[18]"Equations, Tables, and Charts for Compressible Flow," NACA Report 1135, 1953.

[19]"Boundary Layer Integral Matrix Procedure, Version C (BLIMPC)," Aerotherm Report No. UM-70-20, June 22, 1970.

Figure Captions

Fig. 1 Boundary-layer channel. a) Schematic of test section depicting laser access and fluorescence emission ports; b) view of light collection geometry and imaging system.

Fig. 2 Schematic of the experimental arrangement: BCP, beam-combining polarizer cube; WP, half-wave plate; L, lens; BS, beamsplitter; M, mirror; FD, frequency doubler (single-photon only); COLL, collection system; PMT, photomultiplier tube.

Fig. 3 Dual-pulse fluorescence waveform (solid line) and computer-fitted function (dashed line). a) Boundary-layer sample with 100 ppm NO, static pressure = 0.35 atm, T = 172 K; b) room-temperature sample with 5 ppm NO in 0.5 atm N_2, T = 294 K; c) room-temperature reference cell with 500 ppm NO in 0.5 atm N_2, T = 295 K. First pulse is fluorescence from the one-photon Q11 + P21 (18-1/2) excitation; second pulse is from the R21 (7-1/2) excitation. Vertical amplifier bandwidth, 20 MHz; sweep, 50 nsec/div.

Fig. 4 Instrumental temperature error as a function of nitric oxide concentration, using single-photon excitation in a nonflowing cell at ambient temperature: P = 0.5 atm.

Fig. 5 Average temperature distribution through the boundary layer: channel height H = 32.5 mm; M_∞ = 2; T_t = 295 K; T_∞ = 158 K.

Fig. 6 Distribution of rms temperature fluctuations in the boundary-layer using single-photon LIF; y/δ is the location perpendicular to the wall normalized to the boundary-layer thickness. Gas mixture, 100 ppm NO; T_∞ = 158 (Mach 2); δ = 1.4 cm.

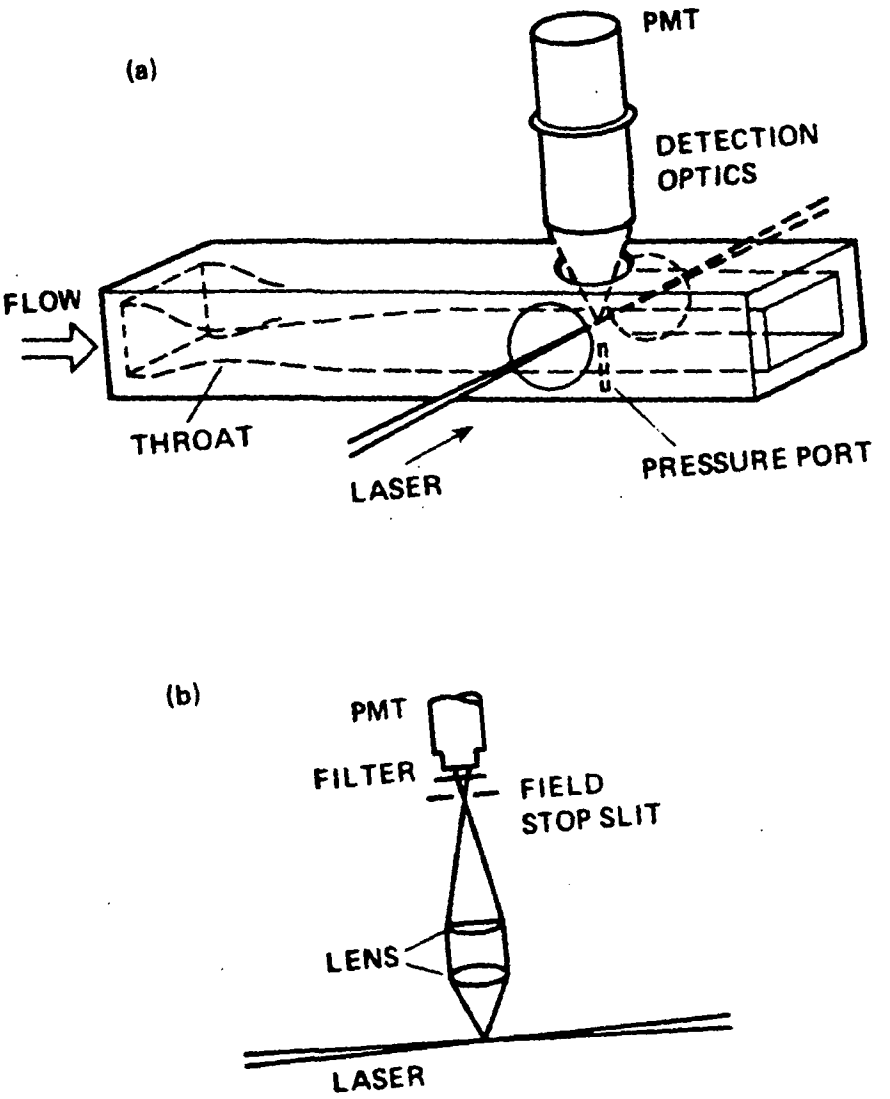
(a)
PMT
DETECTION
OPTICS
FLOW
THROAT
LASER
PRESSURE PORT
(b)
PMT
FILTER
FIELD
STOP SLIT
LENS
LASER

Fig. 1

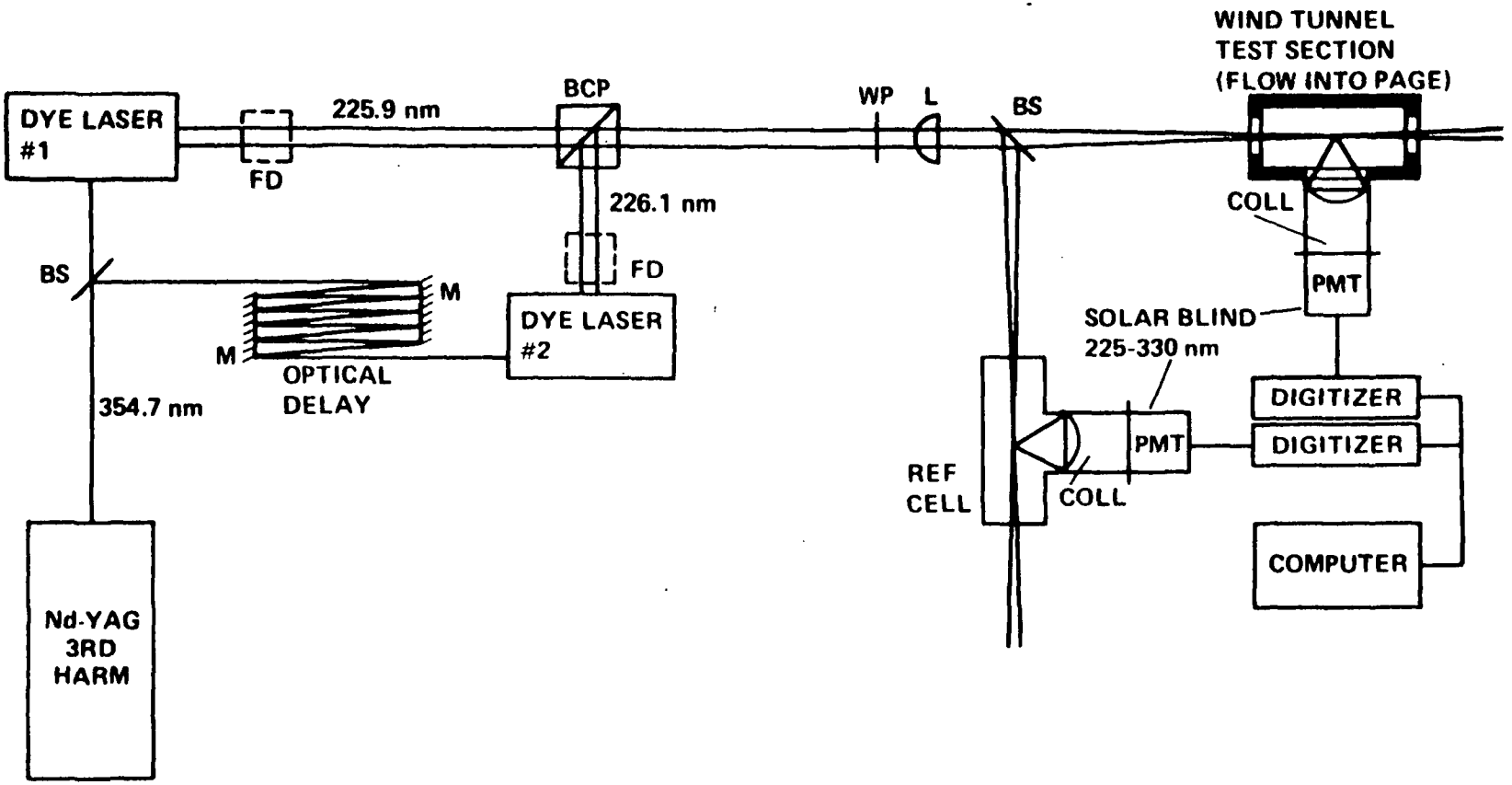
WIND TUNNEL
TEST SECTION
(FLOW INTO PAGE)
DYE LASER
#1
FD
225.9 nm
BCP
WP
L
BS
226.1 nm
FD
COLL
PMT
BS
M
M
OPTICAL
DELAY
DYE LASER
#2
SOLAR BLIND
225-330 nm
354.7 nm
DIGITIZER
DIGITIZER
REF
CELL
COLL
PMT
COMPUTER
Nd-YAG
3RD
HARM

Fig. 2

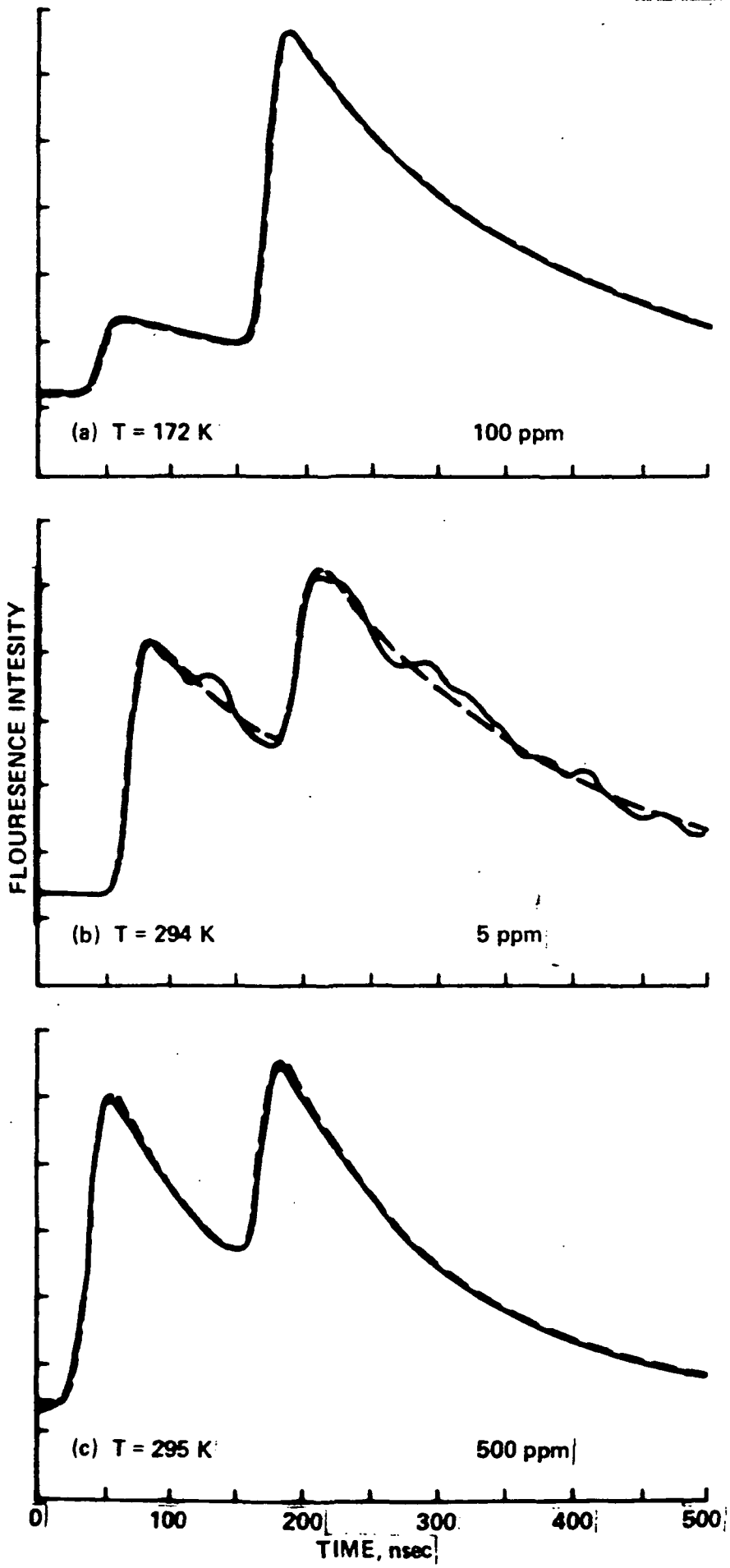
(a) T = 172 K
100 ppm
FLOURESCENCE INTESITY
(b) T = 294 K
5 ppm
(c) T = 295 K
500 ppm
0
100
200
300
400
500
TIME, nsec

Fig. 3

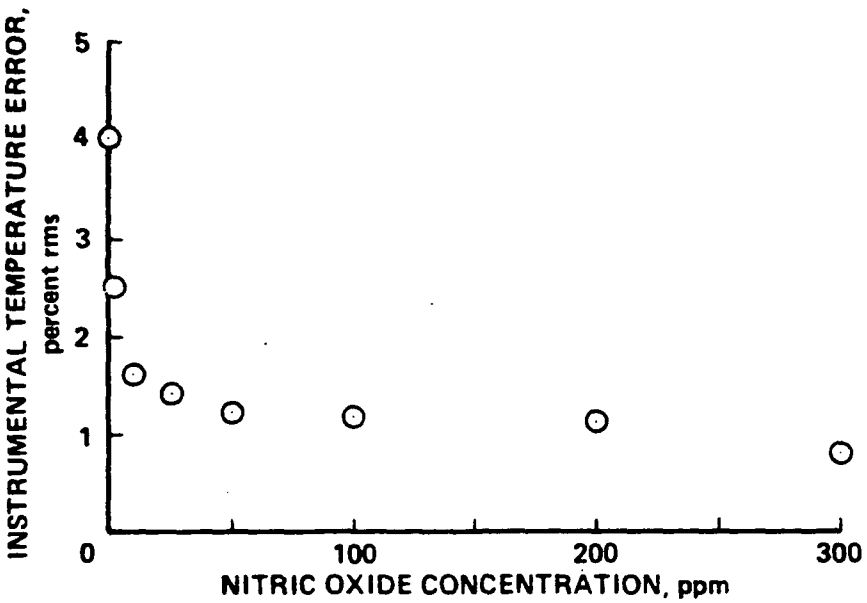
INSTRUMENTAL TEMPERATURE ERROR, percent rms
5
4
3
2
1
0
100
200
300
NITRIC OXIDE CONCENTRATION, ppm

Fig. 4

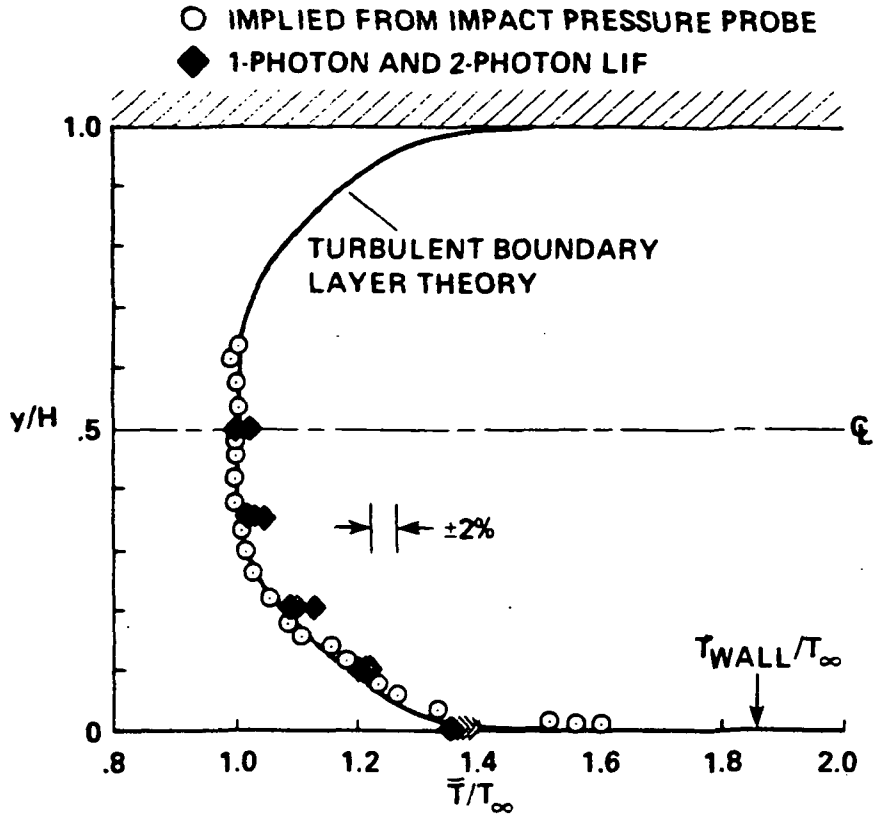
IMPLIED FROM IMPACT PRESSURE PROBE
1-PHOTON AND 2-PHOTON LIF
1.0
TURBULENT BOUNDARY
LAYER THEORY
y/H
.5
℄
±2%
T_{WALL}/T_∞
0
.8
1.0
1.2
1.4
1.6
1.8
2.0
$\bar{T}/T_\infty$

Fig. 5

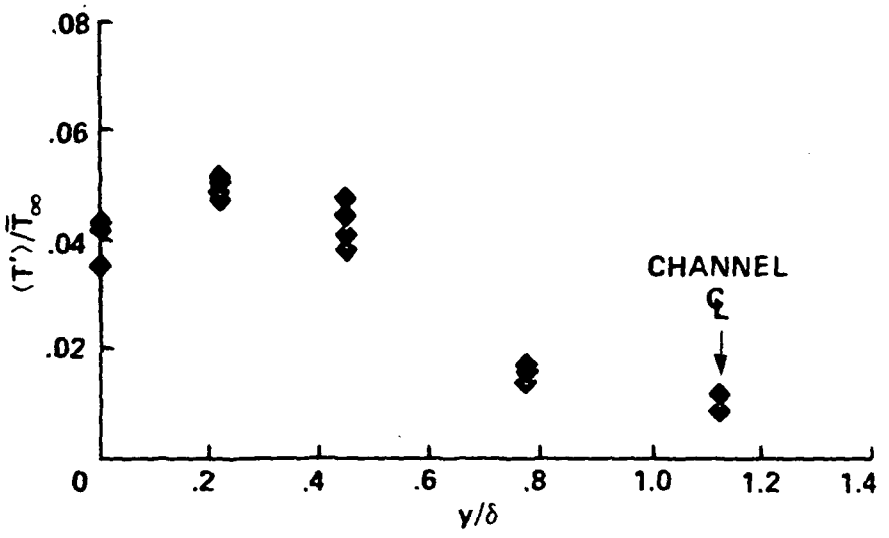
.08
.06
.04
.02
0
$\langle T' \rangle / \bar{T}_\infty$
.2
.4
.6
.8
1.0
1.2
1.4
y/δ
CHANNEL
℄

Fig. 6

"SIMULTANEOUS MEASUREMENTS OF FLUCTUATING TEMPERATURE, DENSITY, AND PRESSURE IN A TURBULENT FLOW USING LASER-INDUCED FLUORESCENCE"

K. P. Gross, Polyatomics Research Institute, 1101 San Antonio Rd., Suite 420, Mountain View, California 94043, (415) 694-6255; R. L. McKenzie, NASA-Ames Research Center, MS 229-1, Moffett Field, California 94035, (415) 694-6158; and P. Logan, Stanford University, Department of Aeronautics and Astronautics, Stanford, California 94305, (415) 694-6255.

ABSTRACT

Quantitative measurements of instantaneous temperature, density, and pressure, obtained simultaneously using pulsed laser-induced fluorescence, have been demonstrated in a supersonic turbulent flow seeded with nitric oxide. The optical measurements agree well with intrusive probe measurement techniques.

SUMMARY:

"Simultaneous Measurements of Fluctuating Temperature, Density, and Pressure in a Turbulent Flow using Laser-Induced Fluorescence"

K. P. Gross, Polyatomics Research Institute, 1101 San Antonio Rd., Suite 420, Mountain View, California 94043, (415) 694-6255; R. L. McKenzie, NASA-Ames Research Center, MS 229-1, Moffett Field, California 94035, (415) 694-6158; and P. Logan, Stanford University, Department of Aeronautics and Astronautics, Stanford, California 94305, (415) 694-6255.

Single-photon laser-induced fluorescence (LIF) has been used to non-intrusively measure all three thermodynamic scalar quantities, temperature, density, and pressure, simultaneously, in a supersonic turbulent nitrogen flow seeded with 100 ppm of nitric oxide.

The experimental method is similar to that described previously [1], and relies on the detection of broadband fluorescence following excitation of two transitions originating from different ground state rotational levels, in the $NO\ ^2\Pi$ (0,0) band. The ratio of fluorescence energies from both transitions is related to the rotational temperature of the gas mixture, whereas the fluorescence from a single transition is related to number density, thus providing a simultaneous measurement of pressure and density. All measurements are made with a temporal resolution of ≈ 125 nsec, and are obtained within a sample volume having dimensions of less than 1 mm.

The flow used to demonstrate these measurements was obtained in a small blowdown wind tunnel facility with a supersonic test section having a cross-section of approximately 3 cm x 6 cm. Sixty-five successive single-pulse